

The reduction of chromate ions by Fe(II) layered hydroxides

S. Loyaux-Lawniczak,^{1,2} Ph. Refait,¹ P. Lecomte,² J.-J. Ehrhardt¹ and J.-M. R. Génin¹

¹ Laboratoire de Chimie Physique pour l'Environnement, UMR 7564 CNRS-Univ. H. Poincaré – Nancy 1, 405, rue de Vandoeuvre, F 54600 Villers-lès-Nancy, France

² Centre National de Recherche sur les Sites et Sols Pollués, 930 Bd Lahure, BP 537, F 59505 Douai cedex.
e-mail address for corresponding author: genin@lcpe.cnrs-nancy.fr

Abstract

The reduction of chromate ions by Fe(OH)₂ and the iron (II)-iron (III) hydroxysulphate green rust, GR(SO₄²⁻), was studied to evaluate whether such synthetic layered hydroxides and the corresponding natural green rust mineral could be involved in the natural attenuation of contaminated environments. The resulting Cr (III) bearing phases, which would govern the subsequent behaviour of chromium, were clearly characterised. Both compounds proved to be very reactive and oxidised instantaneously while chromate ions were reduced to Cr (III) as evidenced by X-ray photoelectron spectroscopy. Mass balance (ICP-AES) demonstrated that the Fe/Cr ratio inside the solid end product was equal to the initial Fe/Cr ratio. The solid phases, analysed by X-ray diffraction, Raman and Mössbauer spectroscopies were identified as Cr-substituted poorly crystallised iron (III) oxyhydroxides in both cases, more precisely δ-FeOOH when starting with Fe(OH)₂ and ferrihydrite when starting with GR(SO₄²⁻).

Introduction

As the use of chromium spread over various industrial applications such as metallurgy, electroplating or tanning of leather, it became a common contaminant in many soils, waste sites and ground and surface waters throughout the world (Richard and Bourg, 1991; Puls *et al.*, 1994). Its most stable oxidation states are Cr (III) and Cr (VI). While Cr (III) is essential in human nutrition, and relatively immobile in the environment, Cr (VI) moves easily through the aquatic media and its compounds are toxic and carcinogenic (Norseth, 1981; Nriagu and Nieboer, 1988; Puls *et al.*, 1994). It is thus clear that redox reactions are very important in the environmental behaviour of chromium.

The capacity for Fe(II) to reduce Cr (VI) in different natural systems is clearly established (e.g. Eary and Rai, 1991; Masscheleyn *et al.*, 1992; Anderson *et al.*, 1994). Several iron (II)-containing minerals had already been considered for laboratory experiments, such as iron (II) sulphide (Patterson *et al.*, 1997) or magnetite (Peterson *et al.*, 1996). The recent discovery of a green rust (GR) compound as a mineral in hydromorphic soils (Trolard *et al.*, 1996, 1997) opens new paths for Cr (VI) reduction by

Fe(II). GRs are very reactive iron (II)-iron (III) hydroxy-compounds where Fe(OH)₂-like sheets alternate with interlayers composed of anions and water molecules. Various types of anions can lead to the formation of a GR, e.g. CO₃²⁻, Cl⁻ or SO₄²⁻. This study investigated the reduction processes of chromate ions CrO₄²⁻ by the iron (II)-iron (III) hydroxysulphate GR(SO₄²⁻) and by the iron (II) hydroxide; it aimed at a first overview of the mechanisms involving this class of layered hydroxides and an accurate identification of the resulting Cr (III)-bearing phases.

Experimental methods

Fe(OH)₂ was precipitated from a 0.23 mol L⁻¹ FeCl₂ · 4 H₂O solution mixed with a 0.4 mol L⁻¹ NaOH solution in a beaker set in a thermostatic bath at 25 ± 0.5 °C. The solutions were not deaerated before precipitation implying that the initial hydroxide was slightly oxidised, containing up to 4% iron (III) as demonstrated previously (Refait and Génin, 1996). The suspension was stirred vigorously during one minute before adding 50 ml of a K₂CrO₄ solution, leading to a total volume of 200 ml. The

amounts of Fe (II) and Cr (VI) were chosen so that the number of electrons provided by the oxidation of Fe (II) to Fe (III) matches the number of electrons consumed during Cr (VI) to Cr (III) reduction, i.e. $\text{Fe (II)}/\text{Cr (VI)} = \text{FeCl}_2 \cdot 4 \text{H}_2\text{O}/\text{K}_2\text{CrO}_4 = 3$, corresponding to a CrO_4^{2-} concentration of 0.08 mol L^{-1} .

Aqueous suspensions of the iron (II)-iron (III) hydroxy-sulphate $\text{GR}(\text{SO}_4^{2-})$ were prepared according to the methodology developed previously (Olowe and Génin, 1991), which involved the oxidation at 25°C of iron (II)-hydroxide in aerated sulphate containing solutions. $\text{Fe}(\text{OH})_2$ was then first precipitated from 0.12 mol L^{-1} $\text{FeSO}_4 \cdot 7 \text{H}_2\text{O}$ and 0.2 mol L^{-1} NaOH solutions and the suspension stirred vigorously to ensure a homogeneous oxidation. The process was monitored by recording the pH and the redox potential E_h of a platinum electrode, using the saturated calomel electrode as reference. The oxidation led after 60 minutes to the complete transformation of $\text{Fe}(\text{OH})_2$ to $\text{GR}(\text{SO}_4^{2-})$ which was ended by a sharp increase of E_h (cf. Fig. 1) and a sharp decrease of pH. Thus, the 50 mL K_2CrO_4 solution was added when these variations occurred. Since the composition of $\text{GR}(\text{SO}_4^{2-})$ is $\text{Fe}^{\text{II}}_4 \text{Fe}^{\text{III}}_2 (\text{OH})_{12} \text{SO}_4 \cdot n \text{H}_2\text{O}$ (Génin *et al.*, 1996), the amount of Cr (VI) added, chosen also to verify $\text{Fe (II)}/\text{Cr (VI)} = 3$, corresponded to $\text{Fe}_{\text{tot}}/\text{Cr (VI)} = (4 + 2)/(4/3) = 9/2$.

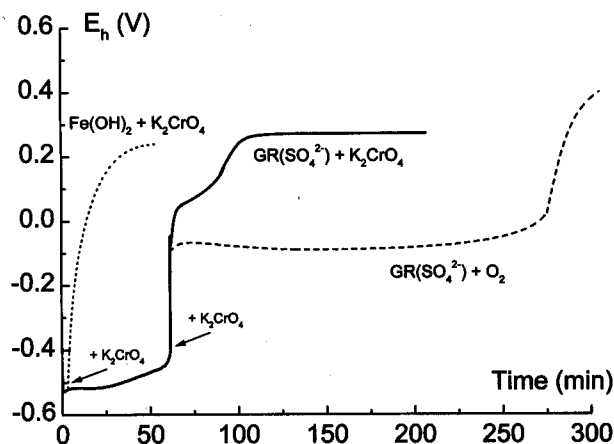


Fig. 1. Electrode potential E_h (standard hydrogen electrode as reference) vs time curves during the following oxidation processes: Aeration of $\text{Fe}(\text{OH})_2$ by stirring a solution containing initially 0.12 mol L^{-1} $\text{FeSO}_4 \cdot 7 \text{H}_2\text{O}$ and 0.2 mol L^{-1} NaOH , addition of CrO_4^{2-} immediately in $\text{Fe}(\text{OH})_2$, addition of CrO_4^{2-} in $\text{GR}(\text{SO}_4^{2-})$.

All chemical products were provided by Prolabo® and verified a 98% minimum purity. After the addition of Cr (VI) to the $\text{Fe}(\text{OH})_2$ or $\text{GR}(\text{SO}_4^{2-})$ suspensions, the redox potential E_h and the pH were monitored. The end products resulting from the reaction between iron (II) species and chromate ions were filtered, dried at room

temperature, ground to powder and analysed by X-ray diffraction (XRD), micro-Raman and Mössbauer spectroscopies. XRD was performed using the $\text{MoK}\alpha_1$ wavelength ($\lambda = 0.70926 \text{ \AA}$). The Raman spectra were recorded using a T64000 triple monochromator and a charge coupled device (CCD) detector. Excitation of the samples was carried out with 632.8 nm radiation from a Spectra Physics® 2017 argon ion laser. The Raman spectra were obtained via a confocal microscope (objective .50; numerical aperture 0.55; spatial resolution of about $3 \mu\text{m}$) in a back scattering geometry. The spectral resolution was of 2 cm^{-1} with a precision on the Raman wavenumber of about 0.3 cm^{-1} . Transmission Mössbauer spectroscopy (TMS) was performed by use of a constant acceleration Mössbauer spectrometer with a 50 mCi source of ^{57}Co in Rh. The spectrometer was calibrated with a $25 \mu\text{m}$ foil of $\alpha\text{-Fe}$ at room temperature. Analyses were performed at 15 K with a closed Mössbauer cryogenic workstation with vibrations isolation stand manufactured by Cryo Industries of America®. Surface analyses were performed by X-ray photoelectron spectroscopy (XPS) using the $\text{MgK}\alpha$ radiation (1253.6 eV), calibrated by means of the C (1s) binding energy of the contamination carbon at 284.6 eV . Chemical analyses were finally performed by ICP-AES. 500 mg of the solids were dissolved using a triacid ($\text{HF} + \text{HClO}_4 + \text{HCl}$) method. Fe and Cr concentrations were calibrated by means of two series of four standard solutions of $\text{FeSO}_4 \cdot 7 \text{H}_2\text{O}$ and K_2CrO_4 dissolved in 5% HCl solutions.

Results and discussion

Oxidation states of Fe and Cr in the end products. The evolutions of the redox potential E_h and pH of the suspensions after the addition of the chromate solution are similar in the case of $\text{Fe}(\text{OH})_2$ and $\text{GR}(\text{SO}_4^{2-})$ as well (Fig. 1). Both E_h and pH present a sharp increase, stabilise rapidly afterwards and do not change any longer. This means that Fe (II) gets oxidised in a few seconds into Fe (III) so that no Fe (II) remains to be oxidised later on by atmospheric O_2 . When Cr (VI) is added to $\text{Fe}(\text{OH})_2$, E_h goes from about -0.5 V to $+0.23 \text{ V}$ (referred to the standard hydrogen electrode) whereas pH varies from about 7.8 to 11.8. When Cr (VI) is added to $\text{GR}(\text{SO}_4^{2-})$, E_h goes from about -0.4 V to $+0.27 \text{ V}$ and pH from about 8 to 10.1. Finally, it must be noted that the kinetics involved by the oxidising action of chromate ions is not comparable to that observed with dissolved oxygen. Whereas a few seconds are sufficient with chromate, the oxidation of $\text{GR}(\text{SO}_4^{2-})$ by dissolved O_2 usually lasts for 2 to 3 hours (Olowe and Génin, 1991 and 1991b; Génin *et al.*, 1996). It is then clear that the action of oxygen can be, in this case, neglected.

The results of the mass balance analyses of Fe and Cr performed by ICP-AES on the final products are listed in Table 1. They show clearly that Cr is present in these

Table 1. Fe and Cr amounts measured by ICP-AES from 500 mg of the two end products.

Initial product	Fe amount (mol kg ⁻¹)	Cr amount (mol kg ⁻¹)	Fe/Cr ratio
Fe(OH) ₂	6.96	2.18	3.19
GR(SO ₄ ²⁻)	7.79	1.71	4.56

products. The Fe/Cr ratios are found at 3.19 when starting from Fe(OH)₂ and 4.56 when starting with GR(SO₄²⁻), values that match the ratios of Fe and Cr initially introduced in solution, that is 3.0 and 4.5. This indicates that the whole amount of chromium is incorporated into the solid matrix.

XPS is a convenient tool to discriminate Cr (VI) from Cr (III). The binding energy of the Cr (2p_{3/2}) line is reported at 577–577.5 eV in Cr (III) oxyhydroxides and hydroxides while it is found at about 580 eV in Cr (VI) salts such as Na₂CrO₄ or Na₂Cr₂O₇ (Allen *et al.*, 1973; Ikemoto *et al.*, 1976; Shuttleworth, 1980). Moreover, the spin-orbit splitting between 2p_{1/2} and 2p_{3/2} peaks is generally reported at 9.7–9.9 eV in Cr (III) compounds and 8.7–9.4 eV in Cr (VI) compounds (Ikemoto *et al.*, 1976). The values obtained with commercial Cr₂O₃ and K₂CrO₄ (Fig. 2), used as references, are in good agreement with the literature. Looking at the Cr (2p) spectra of the end products presented in Fig. 2, it can be seen that in each case,

the Cr (2p_{3/2}) or Cr (2p_{1/2}) line could be adjusted with only one component, implying that almost all Cr atoms (> 95%) were in the same oxidation state. The corresponding Cr (2p_{3/2}) binding energies are found close to 577.2 eV, and the 2p spin-orbit splits at 9.8 eV, values characteristic of Cr (III).

Identification of the end products. The XRD patterns obtained (Fig. 3) are typical of poorly crystallised compounds. The end product of Fe(OH)₂ displays four diffraction lines that allow it to be identified as a δ-FeOOH-like oxyhydroxide (Francombe and Rooksby, 1959). This is not surprising, as δ-FeOOH is the compound usually obtained by addition of hydrogen peroxide H₂O₂ to Fe(OH)₂ suspensions, a process resulting in an instantaneous and violent oxidation of Fe (II) (Glemser and Gwinner, 1939). The δ-FeOOH sample used as a reference for the XRD analyses (Fig. 3) was prepared accordingly.

The end product obtained from GR(SO₄²⁻) is even more poorly crystallised. Only two diffraction lines can be distinguished, at about 0.255 nm and 0.148 nm. Such a diffraction pattern is typical of the so-called '2-line ferrihydrite' (e.g. Carlson and Schwertmann, 1981). Ferrihydrite is the least crystalline of the hydrous iron oxides and oxyhydroxides and even its stoichiometry, often assumed at Fe₅HO₈ · 4H₂O (Towe and Bradley, 1967), is somewhat uncertain. Its XRD pattern varies with crystallinity; poorly crystalline samples lead to only two broad diffraction peaks whereas better crystalline samples can

Solids obtained after chromate reduction

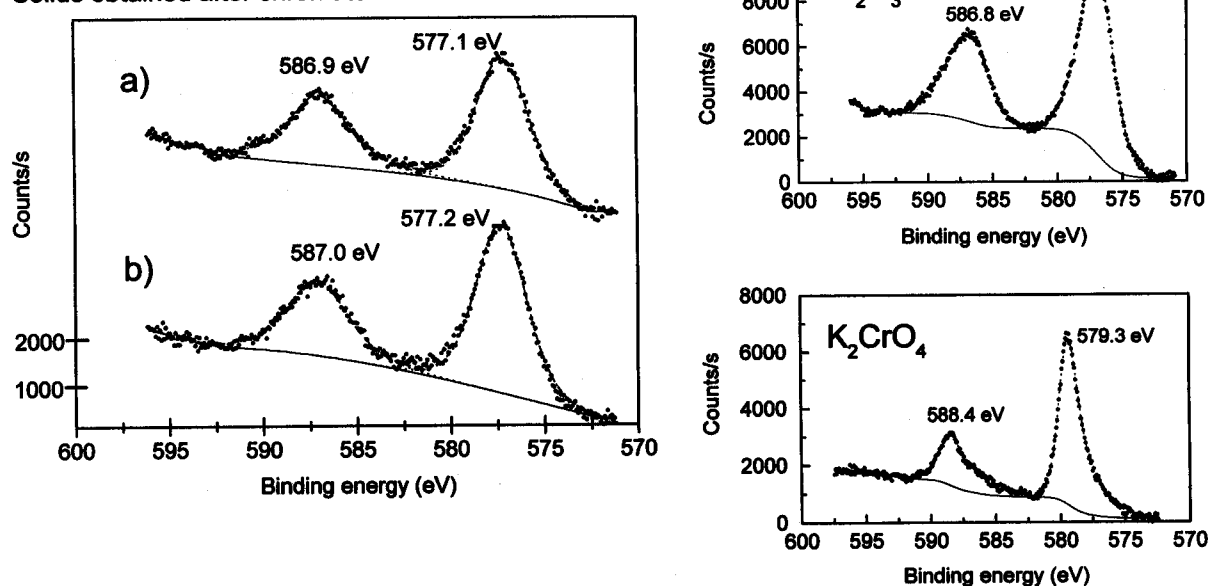


Fig. 2. XPS analyses of the end products compared with those of Cr₂O₃ and K₂CrO₄: Cr 2p spectra. (a) obtained from Fe(OH)₂ and (b) obtained from GR(SO₄²⁻).

•••: experimental curve. ----: individual peaks. —: background.

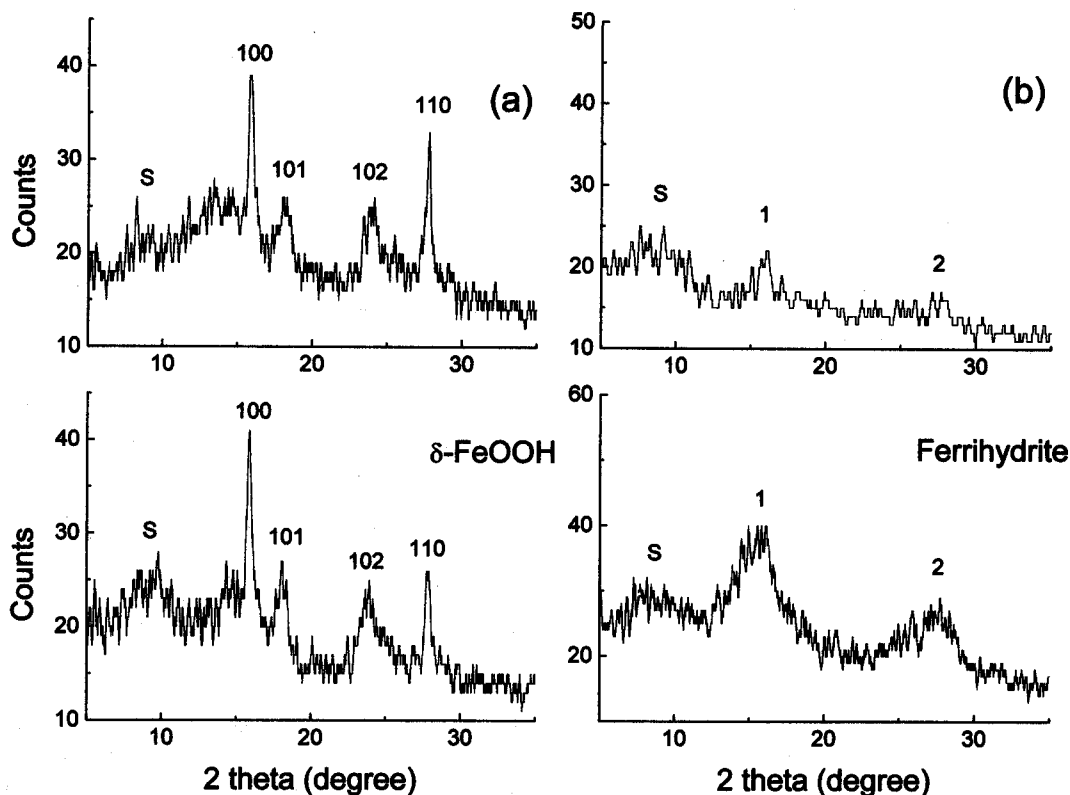


Fig. 3. XRD patterns of the end products using the $MoK\alpha_1$ wavelength ($\lambda = 0.70926 \text{ \AA}$) compared with standard patterns of $\delta\text{-FeOOH}$ and 2-line ferrihydrite.

(a) obtained from $Fe(OH)_2$ and (b) obtained from $GR(SO_4^{2-})$.

The broad peak S is due to the adhesive tape on which the samples are fixed, 1 and 2 are the diffraction lines of the '2-line ferrihydrite'. Other lines are that of $\delta\text{-FeOOH}$, indexed according to Francombe and Rooksby, (1959).

display up to six peaks. The reference sample of 2-line ferrihydrite (Fig. 3) was prepared according to the method described by Cornell and Schwertmann (1996).

Mössbauer spectra of the end products obtained after chromate reduction are presented in Fig. 4. Two sextets S_1 and S_2 were used to fit the experimental curve of the

$\delta\text{-FeOOH}$ compound resulting from the oxidation of $Fe(OH)_2$. The corresponding hyperfine parameters, listed in Table 2, are consistent with those quoted in the literature (Persoons *et al.*, 1986 ; Pollard and Pankhurst, 1991). Both sextets are characterised by nil quadrupole splitting ΔE_Q and large hyperfine fields H of 509 and 469 kOe. The

Table 2. Mössbauer hyperfine parameters measured at 15 K of the end products.

δ = isomer shift with respect to metallic α -iron at room temperature in $mm \text{ s}^{-1}$; ΔE_Q = quadrupole splitting in $mm \text{ s}^{-1}$; H = hyperfine field in kOe; RA = relative abundance in %; Γ = full width at half maximum in $mm \text{ s}^{-1}$.

	(a) Product obtained from $Fe(OH)_2$					(b) Product obtained from $GR(SO_4^{2-})$				
Site	δ	ΔE_Q	H	RA	Γ	δ	ΔE_Q	H	RA	Γ
S_1	0.50	0	509	74	0.85	0.50	0	489	53	0.8
S_2	0.50	0	469	26	0.85	0.49	0	456	34	0.8
S_3	—	—	—	—	—	0.46	0	412	13	0.8

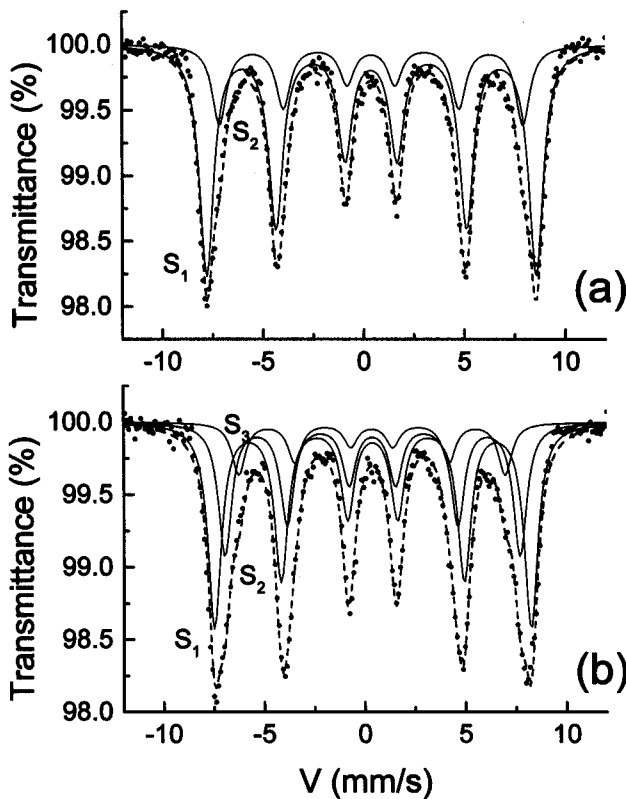


Fig. 4. TMS spectra measured at 15 K of the end products. (a) obtained from $\text{Fe}(\text{OH})_2$ and (b) obtained from $\text{GR}(\text{SO}_4^{2-})$. \cdots : experimental curve. $-\cdots-$: elementary components. $—$: global computed curve.

compound resulting from the oxidation of $\text{GR}(\text{SO}_4^{2-})$ exhibits a different spectrum. Firstly, an additional sextet S_3 had to be used in order to reach a satisfactory fit of the experimental curves. Secondly, the sextets are characterised by smaller H values, the maximum being observed for example at 490 kOe vs 509 kOe. The presence of these various sextets must be interpreted as a distribution of hyperfine fields due to poor crystallinity rather than three distinct sites. The maximum absorption is observed near 480 kOe, a value indeed typical of ferrihydrite (Murad and Schwertmann, 1980).

Micro-Raman spectroscopy study and formation of Cr-substituted Fe(III)-oxyhydroxides (Fig. 5). The literature concerning Raman studies of δ - FeOOH and ferrihydrite is scarce. In particular, no reference concerning ferrihydrite could be found. According to de Faria *et al.* (1997), the Raman spectrum of δ - FeOOH is mainly composed of two broad bands around 400 and 700 cm^{-1} , a description consistent with the spectrum of the end product obtained from $\text{Fe}(\text{OH})_2$. Nevertheless, the band at 700 cm^{-1} rather appears as the superimposition of three distinct bands at 582, 670 and 705 cm^{-1} . In contrast, the spectrum of ferrihydrite displays only two bands at 415 and 705 cm^{-1} . But the most interesting fact is that the bands characterising these iron (III) compounds are the only bands present. More precisely, neither the band of $\text{Cr}(\text{OH})_3$ at 525 cm^{-1} (Melendres *et al.*, 1992) nor those of Cr_2O_3 at about 300, 350, 550 and 610 cm^{-1} (Zuo *et al.*, 1996) can be seen, implying that Cr (III) is incorporated in each case in the iron (III) compound. To confirm it, micro-Raman analyses were performed on various spots of the samples, and always led to the same spectrum. This homogeneity was also confirmed by the optical observations through the microscope.

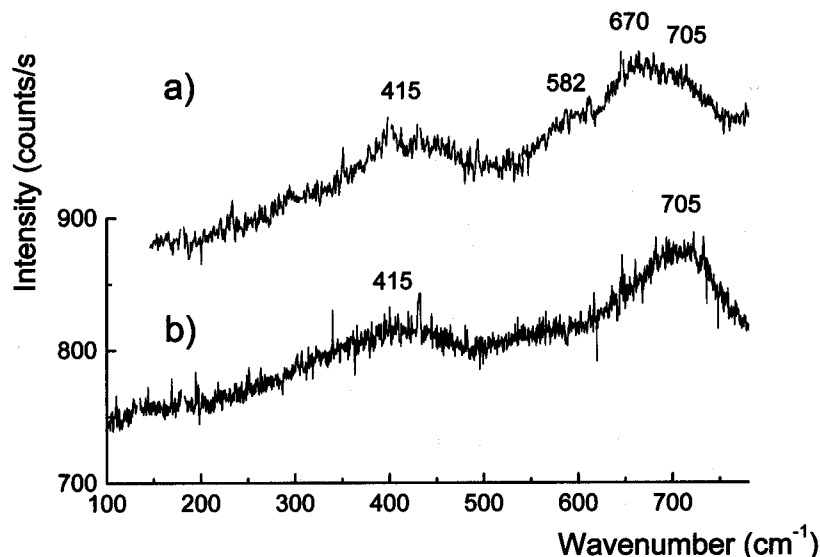


Fig. 5. Raman spectra of the end products. (a) obtained from $\text{Fe}(\text{OH})_2$ and (b) obtained from $\text{GR}(\text{SO}_4^{2-})$.

The chemical composition of the solid phases obtained at the end of the overall oxydoreduction processes can then be written as follows :

If starting with $\text{Fe}(\text{OH})_2$: $\delta\text{-Fe}_{3/4}\text{Cr}_{1/4}\text{OOH}$

If starting with $\text{GR}(\text{SO}_4^{2-})$: $\text{Fe}_{45/11}\text{Cr}_{10/11}\text{HO}_8 \cdot 4\text{H}_2\text{O}$

Topotactic relationships between initial and end products.

It is well known from the work of Francombe and Rooksby (1959) that the crystal structure of $\delta\text{-FeOOH}$ is closely related to that of $\text{Fe}(\text{OH})_2$. This structure consists of an hexagonal close packed array of oxygen atoms with a stacking sequence ABAB... The Fe(II) ions of $\text{Fe}(\text{OH})_2$ occupy half of the octahedral sites by leaving every other plane completely empty, leading to the $\text{AcB}\square\text{A}...$ stacking sequence where A,B are the planes of oxygen atoms, c those of iron atoms and \square the empty octahedral sites. In the case of $\delta\text{-FeOOH}$, the Fe organisation among the available octahedral sites is different and various models were proposed (Okamoto, 1968; Patrat *et al.*, 1983; Drits *et al.*, 1993b). The transformation of $\text{Fe}(\text{OH})_2$ into $\delta\text{-FeOOH}$ is then topotactic in character and involves an *in situ* oxidation of Fe (II) ions inside the crystal followed by a deprotonation of the OH^- ions into O^{2-} and minor rearrangements of the positions of the iron (III) ions. The appearance of this peculiar phase indicates that the oxidation does not involve a dissolution-precipitation mechanism. The reduction of Cr (VI) would then be a surface reaction rather than one which occurs by dissolved iron (II) complexes.

To some extent, GR compounds are also structurally similar to $\text{Fe}(\text{OH})_2$. Since the work of Stampfl (1969), it was generally admitted that these compounds were layered hydroxides of the pyroaurite-sjögrenite group. They are characterised by a crystal structure in which $\text{Fe}(\text{OH})_2$ like hydroxide sheets, positively charged due to the presence of Fe (III) cations, e.g. $[\text{Fe}^{\text{II}}_4\text{Fe}^{\text{III}}_2(\text{OH})_{12}]^{2+}$, alternate regularly with negatively charged interlayers made of anions and water molecules, e.g. $[\text{SO}_4 \cdot n\text{H}_2\text{O}]^{2-}$. Therefore, when $\text{AcB}\square$ is the elementary stratum in $\text{Fe}(\text{OH})_2$, AcBi , where *i* is the intercalated layer, is the elementary stratum in a GR compound. Finally, the '2-line ferrihydrite' corresponds to a poorly ordered material. A recent detailed structural model has been proposed (Drits *et al.*, 1993a) but it can be considered, for simplifying, that the crystal structure would consist only of planar arrangements of $\text{Fe}(\text{O}, \text{OH}, \text{OH}_2)_6$ octahedra without any precise stacking.

The action of hydrogen peroxide on GR compounds has already been described (Bernal *et al.*, 1959; Refait and Génin, 1993). It is similar to what is observed with $\text{Fe}(\text{OH})_2$, the XRD pattern of the resulting end product showing the lines of $\delta\text{-FeOOH}$ plus an extra, very sharp line corresponding to the distance *d* between Fe planes, e.g. $d \sim 8 \text{ \AA}$ in $\text{GR}(\text{Cl}^-)$ and $d \sim 11 \text{ \AA}$ in $\text{GR}(\text{SO}_4^{2-})$. The presence of this line proves that the intercalated anions of the GR are trapped inside the interlayers of the crystal structure during the process. The end product of the oxidation of $\text{GR}(\text{SO}_4^{2-})$ by chromate ions is different and

clearly identified as ferrihydrite, which would imply that the intercalated sulphate ions are removed from the crystal. This is the main difference between the action of H_2O_2 and the action of CrO_4^{2-} ions. This suggests that part of the chromate ions, very similar to SO_4^{2-} , could substitute for the sulphate ions inside the interlayers before being reduced. The kinetics of this substitution is unknown and it is impossible to evaluate what proportion of the overall amount of CrO_4^{2-} could be involved in this process. Such a mechanism, even though it would concern only a minor part of the chromate anions, would however explain (i) the rejection of SO_4^{2-} and (ii) the destruction of the original well defined stacking sequence of $\text{GR}(\text{SO}_4^{2-})$ giving the disordered stacking of ferrihydrite and, (iii) the presence of Cr (III) in such an iron (III) compound.

Concluding remarks. The conditions of these laboratory experiments differ from what could be found in natural aquifers, especially concerning the nature and cristallinity of the compounds (Génin *et al.*, 1998) and the chromium and iron concentrations. In contrast, the groundwater of contaminated industrial sites can contain hexavalent chromium with concentrations similar or even greater than those chosen here (Henderson, 1994 ; Baron *et al.*, 1996). Nevertheless, it is clearly demonstrated that the reactivity of iron (II) containing layered hydroxycoumpounds towards Cr (VI) is very important. The redox processes produce unusual iron (III)-based phases inside which large proportions of Cr (III) can be incorporated.

References

- Allen, G.C., Curtis, M.T., Hooper, A.J. and Tucker, P.M., 1973 X-ray photoelectron spectroscopy of chromium-oxygen systems. *J. Chem. Soc., Dalton Trans.* 1675-1683.
- Anderson, L.D., Kent, D.B. and Davis, J.A., 1994. Batch experiments characterising the reduction of chromium VI using suboxic material from a mildly reducing sand and gravel aquifer. *Environ. Sci. Technol.* 28, 178-185.
- Baron, D., Palmer, C.D. and Stanley, J.T., 1996. Identification of two iron-chromate precipitates in a Cr(VI)-contaminated soil. *Environ. Sci. Technol.* 30, 964-968.
- Bernal, J.D., Dasgupta, D.R. and Mackay, A.L., 1959. The oxides and hydroxides of iron and their structural interrelationships. *Clay Min. Bull.* 4, 15-30.
- Carlson, L. and Schwertmann, U., 1981. Natural ferrihydrites in surface deposits from Finland and their association with silica. *Geochim. Cosmochim. Acta* 45, 421-429
- Cornell R. M. and Schwertmann, U., 1996. *The iron oxides. Structure, properties, reactions, occurrences and uses.* VCH, Weinheim, p. 491.
- Drits, V.A., Sakharov, B.A., Salyn, A.L. and Manceau, A., 1993a. Structural model for ferrihydrite. *Clay Miner.* 28, 185-207.
- Drits, V.A., Sakharov, B.A. and Manceau, A., 1993b. Structure of feroxyhyte as determined by simulation of X-ray diffraction curves. *Clay Miner.* 28, 209-222.

- Eary, L.E. and Rai, D., 1991. Chromate reduction by subsurface soils under acidic conditions. *Soil Sci. Soc. Am. J.* **55**, 676–683.
- de Faria, D.L.A., Venancio, S. and de Oliveira, M.T., 1997. Raman spectroscopy of some iron oxides and oxyhydroxides. *J. Raman Spectroscopy* **28**, 873–878.
- Francombe, M.H. and Rooksby, H.P., 1959. Structure transformations effected by dehydration of diasporite, goethite and delta ferric oxide. *Clay Min. Bull.* **4**, 1–14.
- Génin, J.-M.R., Olowe, A.A., Refait, Ph. and Simon, L., 1996. On the stoichiometry and Pourbaix diagram of Fe(II)–Fe(III) hydroxy-sulphate or sulphate-containing green rust 2; an electrochemical and Mössbauer spectroscopy study. *Corros. Sci.* **38**, 1751–1762.
- Génin, J.-M.R., Bourrié, G., Trolard, F., Abdelmoula, M., Jaffrezic, A., Refait, Ph., Maître, V., Humbert, B. and Herbillon, A., 1998. Thermodynamic equilibria in aqueous suspensions of synthetic and natural Fe(II)–Fe(III) green rusts: occurrences of the Mineral in hydromorphic soils. *Environ. Sci. Technol.* **32**, 1058–1068.
- Glemser, O. and Gwinner, E., 1939. Über eine neue ferromagnetische Modifikation des Eisen(III)-Oxydes. *Z. Anorg. Chem.* **240**, 163–171.
- Henderson, T., 1994. Geochemical reduction of hexavalent chromium in the Trinity Sand aquifer. *Ground Water* **32**, 477–486.
- Ikemoto, I., Ishii, K., Kinoshita, S., Kuroda, H., Franco, M.A.A. and Thomas, J.M., 1976. X-ray photoelectron spectroscopic studies of CrO₂ and some related chromium compounds. *J. Solid State Chem.* **17**, 425–430.
- Masscheleyn, P.H., Pardue, J.H., DeLaune, R.D. and Patrick, W.H.Jr., 1992. Chromium redox chemistry in a lower Mississippi valley bottomland hardwood wetland. *Environ. Sci. Technol.* **26**, 1217–1226.
- Melendres, C.A., Pankuch, M., Li, Y.S. and Knight, R.L., 1992. Surface enhanced Raman spectroelectrochemical studies of the corrosion films on iron and chromium in aqueous solution environments. *Electrochim. Acta* **37**, 2747–2754.
- Murad, E. and Schwertmann, U., 1980. The Mössbauer spectrum of ferrihydrite and its relations with those of other iron oxides. *Amer. Min.* **65**, 1044–1049.
- Norseth, T., 1981. The carcinogenicity of chromium. *Environmental Health Perspectives* **40**, 121–130.
- Nriagu, J.O. and Nieboer, E. *Chromium in the natural and human environments*; John Wiley and Sons, New York, 1988.
- Okamoto, S., 1968. Structure of δ -FeOOH. *J. Am. Ceram. Soc.* **51**, 594–599.
- Olowe, A.A. and Génin, J.-M.R., 1991a. The mechanism of oxidation of Fe(II) hydroxide in sulphated aqueous media: importance of the initial ratio of the reactants. *Corros. Sci.* **32**, 965–984.
- Olowe, A.A., Refait, Ph. and Génin, J.-M.R., 1991b. Influence of concentration on the oxidation of ferrous hydroxide in basic sulphated medium: particle size analysis of goethite and delta FeOOH. *Corros. Sci.* **32**, 1003–1020.
- Patrat, G., de Bergevin, F. and Joubert, J.C., 1983. Structure locale de δ -FeOOH. *Acta Cryst.* **B39**, 165–170.
- Patterson, R.R., Fendorf, S. and Fendorf, M., 1997. Reduction of hexavalent chromium by amorphous iron sulfide. *Environ. Sci. Technol.* **31**, 2039–2044.
- Persoons, R.M., Chambaere, D.G. and de Grave, E., 1986. Mössbauer effect study of the magnetic structure in δ -FeOOH. *Hyp. Int.* **28**, 647–650.
- Peterson, M.L., Brown, G.E. Jr. and Parks, G.A., 1996. Direct XAFS evidence for heterogeneous redox reaction at the aqueous chromium magnetite interface. *Colloids Surf. A* **107**, 77–78.
- Pollard, R.J. and Pankhurst, Q.A., 1991. Ferrimagnetism in fine ferroxhyte particles. *J. Magn. Magn. Mat.* **99**, L39–L44.
- Puls, R.W., Clark, D.A., Paul, C.J. and Vardy, J., 1994. Transport and transformation of hexavalent chromium through soils and into ground water. *J. Soil Contamination* **3**, 203–224.
- Refait, Ph. and Génin, J.-M.R., 1993. The oxidation of Ni(II)–Fe(II) hydroxides in chloride-containing aqueous media. *Corros. Sci.* **34**, 2059–2070.
- Refait, Ph. and Génin, J.-M.R., 1996. Chloride-containing ferrous hydroxides. *SIF Conference Proceedings* **50**, 55–58.
- Richard, F.C. and Bourg, A.C.M., 1991. Aqueous geochemistry of chromium: a review. *Wat. Res.* **25**, 807–816.
- Shuttleworth, D., 1980. Preparation of metal-polymer dispersions by plasma techniques. An ESCA investigation. *J. Phys. Chem.* **84**, 1629–1634.
- Stampfl, P.P., 1967. Ein basisches Eisen II–III Karbonat in Rost. *Corros. Sci.* **9**, 185–187, 1969.
- Towe, K.M. and Bradley, W.F., 1967. Mineralogical constitution of colloidal ‘hydrated ferric oxides’. *J. Colloid Interface Sci.* **24**, 384–392.
- Trolard, F., Abdelmoula, M., Bourrié, G., Humbert, B. and Génin, J.-M.R., 1996. Evidence of the occurrence of a ‘Green Rust’ component in hydromorphic soils—Proposition of the existence of a new mineral: ‘fougerite’. *Compt. Rend. Acad. Sci.* **323 Série IIA**, 1015–1022.
- Trolard, F., Génin, J.-M.R., Abdelmoula, M., Bourrié, G., Humbert, B. and Herbillon, A.J., 1997. Identification of a green rust mineral in a reductomorphic soil by Mössbauer and Raman spectroscopies. *Geochim. Cosmochim. Acta* **61**, 1107–1111.
- Zuo, J., Xu, C., Hou, B., Wang, C., Xie, Y. and Qian, Y., 1996. Raman spectra of nanophase Cr₂O₃. *J. Raman Spectrosc.* **27**, 921–923.